ELSEVIER

Journal of Organometallic Chemistry 526 (1996) 341–350

Journal of Organometallic Chemistry

Rhodium(I) complexes with hydrotris(3-phenylpyrazol-1-yl)borate ligand Tp^{Ph}: X-ray crystal structures of $Tp^{Ph}Rh(NBD)$ and $Tp^{Ph}Rh(COD)$

D. Sanz [a], M.D. Santa María [a], R.M. Claramunt [a,*], M. Cano [b,*], J.V. Heras [b], J.A. Campo [b], F.A. Ruíz [b], E. Pinilla [b], A. Monge [c]

[a] *Departamento de Química Orgánica y Biología, Facultad de Ciencias, Universidad Nacional de Educación a Distancia, Senda del Rey s/n, E-28040 Madrid, Spain*

[b] *Departamento de Química Inorgánica I, Facultad de Ciencias Químicas, Universidad Complutense, E-28040 Madrid, Spain*

[c] *Instituto de Ciencias de los Materiales sede D, CSIC, Serrano 113, Laboratorio de Difracción de Rayos-X, Cristalografía, Facultad de Ciencias Químicas, Universidad Complutense, E-28040 Madrid, Spain*

Received 1 May 1996; revised 6 June 1996

Abstract

Solution studies by ^{1}H and ^{13}C NMR and IR spectroscopy of rhodium(I) complexes $Tp^{Ph}Rh(NBD)$ **1**, $Tp^{Ph}Rh(COD)$ **2** and $Tp^{Ph}Rh(CO)_2$ **3** (NBD = 2,5-norbornadiene, COD = 1,5-cyclooctadiene) show that these compounds exist as mixtures of two isomeric square-planar complexes containing the Tp^{Ph} ligand in a bidentate k^2-bonded form, with the third uncoordinated pyrazolyl ring occupying an equatorial position, form **A**, or an axial position, form **B**. In the solid state the complexes are tetracoordinated, as proved by X-ray crystallography: **1** (monoclinic, space group $P2_1/c$) and **2** (orthorhombic, space group $P2_12_12_1$), whose structures correspond to forms **B** and **A** respectively. Changes in the **A**/**B** ratio in the solid complex $Tp^{Ph}Rh(CO)_2$ **3** were observed after several months.

Keywords: Trispyrazolylborates; Rhodium complexes; NMR spectroscopy; Crystal structures

1. Introduction

Trispyrazolylborate anions are versatile ligands in coordination chemistry, since depending on the electronic and steric effects of the pyrazole substituents and the electron-donating character of the ancillary ligands they behave as tridentate or bidentate ligands [1–5]. Recently, Venanzi and coworkers [6–8] have described several examples in which variations of trispyrazolylborate denticity occur in Rh(I) and Ir(I) complexes, the characterisation being achieved by IR and NMR spectroscopy and, in a few cases, by X-ray diffraction.

This paper describes the synthesis and behaviour of two new rhodium(I) complexes of hydrotris(3-phenylpyrazol-1-yl)borate ligand Tp^{Ph}, $Tp^{Ph}Rh(LL)$ [LL = NBD, COD] **1**, **2**, and affords new insights into the case of the previously known $Tp^{Ph}Rh(CO)_2$ **3** [2]. The dynamic equilibrium among three isomeric forms will also be discussed: **A**, a square-planar complex with two coordinated pyrazolyl groups and the uncoordinated one in equatorial position; **B**, a square-planar complex with two coordinated pyrazoles and the third one in axial position; **C**, a five-coordinated complex with a k^3-bonded trispyrazolylborate ligand (see Scheme 1). The energy differences between the forms **A**, **B** and **C** should be small, as two or three isomers can be detected simultaneously.

2. Experimental details

2.1. Synthesis of rhodium(I) complexes

2.1.1. General

Literature methods were used to prepare 3(5)-phenylpyrazole [9,10] and the hydrotris(3-phenylpyrazol-1-yl)borate [10]. The organometallic starting materials $Rh_2Cl_2(NBD)_2$ and $Rh_2Cl_2(COD)_2$ were obtained as described in Refs. [11,12]. All reactions were performed

* Corresponding authors.

PII S0022-328X(96)06577-1

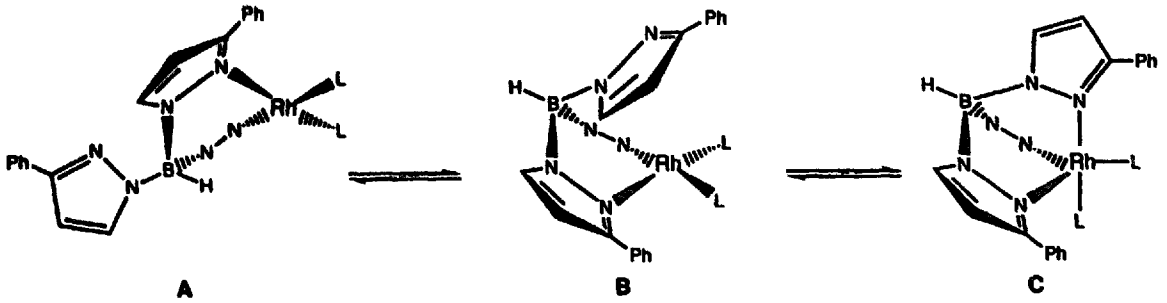

Scheme 1.

at room temperature, and an inert atmosphere was not necessary. Commercial solvents were dried prior to use.

Elemental analyses for carbon, hydrogen and nitrogen were carried out by the Microanalytical Service of the Complutense University of Madrid. IR spectra were recorded either as KBr discs or in solution in NaCl cells on an FT-IR Nicolet Magna 550 spectrometer.

2.1.2. [Rh(Tp^{Ph})(diolefine)] 1 and 2

To a solution of $Rh_2Cl_2(diolefine)_2$ (diolefine = NBD, COD) (0.2 mmol) in dichloromethane (15 ml) was added 0.4 mmol of Tp^{Ph} ligand. The clear yellow–orange solution was stirred for 2 h and the solvent was then removed at reduced pressure. The solid residue was dissolved in 5 ml of dichloromethane and the solution filtered through Celite. The solution was evaporated off and then the yellow–orange solid treated with diethyl ether, the solvent evaporated off again and the solid dried under vacuum.

[Rh(Tp^{Ph})(NBD)] 1. Anal. Found. C, 64.06; H, 4.67; N, 13.1. $RhBC_{34}H_{30}N_6$ Calc.: C, 64.16; H, 4.76; N, 13.21%.

[Rh(Tp^{Ph})(COD)] 2. Anal. Found: C, 64.41; H, 5.14; N, 12.93. $RhBC_{35}H_{34}N_6$ Calc.: C, 64.42; H, 5.26; N, 12.88%.

2.1.3. [Rh(Tp^{Ph})(CO)$_2$] 3

Carbon monoxide was bubbled for 45 min through a solution of [Rh(Tp^{Ph})(diolefine)] 1 or 2 (0.1 mmol) in dichloromethane (15 ml) at room temperature and atmospheric pressure. The yellow solid obtained after removal of the solvent was treated with diethyl ether and evaporated again to dryness. The yellow solid was dried under vacuum. Anal. Found: C, 58.65; H, 3.82; N, 14.25. $RhBC_{29}H_{22}N_6O_2$ Calc.: C, 58.02; H, 3.70; N, 14.0%.

2.2. NMR spectroscopy

Nuclear magnetic resonance spectra were obtained on a Bruker AC-200 spectrometer at 24 °C unless otherwise indicated. ^1H and ^{13}C chemical shifts (ppm) are downfield from tetramethylsilane (TMS) using $CDCl_3$ (δ^1H = 7.26 ppm, $\delta^{13}C$ = 77.0 ppm) and DMSO-d_6 (δ^1H = 2.49 ppm, $\delta^{13}C$ = 39.5 ppm) as internal standards. ^1H (10^{-2} M solutions) and ^{13}C (10^{-1} M solutions) chemical shifts are accurate to 0.01 and 0.1 ppm respectively; coupling constants are accurate to ±0.2 Hz (^1H NMR) and ±0.6 Hz (^{13}C NMR). Homonuclear (^1H–^1H) and heteronuclear (^1H–^{13}C) correlation experiments were carried out with standard procedures [13]. See Fig. 1 for NMR atomic numbering.

2.3. X-ray diffraction

Yellow prismatic crystals were obtained for both compounds $Tp^{Ph}Rh(NBD)$ 1 and $Tp^{Ph}Rh(COD)$ 2 from dichloromethane/diethyl ether. The data were collected on an Enraf–Nonius CAD4 diffractometer and unit cell constants were refined from least-squares fitting of the Θ values of 25 reflections with $12° \leq 2\Theta \leq 23°$ for 1 and $15° \leq 2\Theta \leq 24°$ for 2. A summary of the fundamental crystal data for both compounds is given in Table 1.

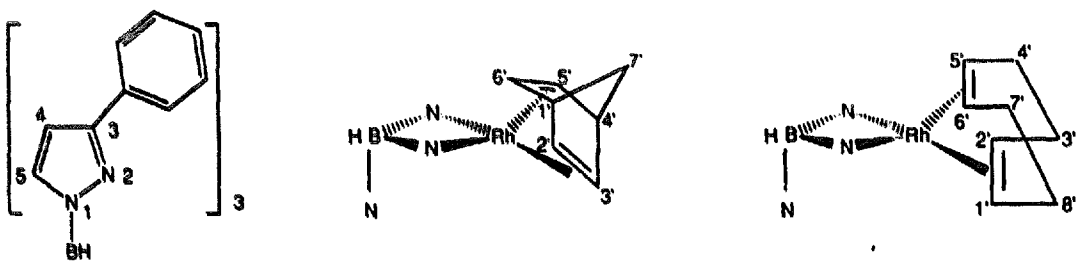

Fig. 1. Atomic numbering used in the NMR assignments.

Table 1
Crystal and refinement data for [Tp^{Ph}Rh(NBD)] (1) and [Tp^{Ph}Rh(COD)] (2)

Formula	$BN_6C_{34}H_{30}Rh$	$BN_6C_{35}H_{35}Rh$
M_r	636.37	652.41
Crystal system	monoclinic	orthorhombic
Space group	$P2_1/c$	$P2_12_12_1$
a (Å)	10.096(2)	9.492(3)
b (Å)	19.458(3)	10.632(3)
c (Å)	15.041(2)	30.893(4)
β (°)	92.54(1)	
V Å^3	2951.4(8)	3117(1)
Z	4	4
F(000)	304	1344
ρ(calc) (g cm^{-3})	1.43	1.39
T (K)	295	295
μ (cm^{-1})	6.0	5.7
Crystal dimensions (mm^3)	0.25 × 0.2 × 0.25	0.2 × 0.25 × 0.25
Diffractometer	Enraf–Nonius CAD4	Enraf–Nonius CAD4
Radiation	graphite-monochromated Mo Kα (λ = 0.71069 Å)	graphite-monochromated Mo Kα (λ = 0.71069 Å)
Scan technique	ω–2θ	ω–2θ
Data collected	(−12,0,0) to (12,23,27)	(0,0,0) to (11,12,36)
θ (°)	$1 < \theta < 25$	$1 < \theta < 25$
Unique data	5165	3118
Unique data (I) ≥ 2σ(I)	3842	2652
R(int) (%)	0.8	
Standard reflections	3/222	3/141
R_F (%)	2.7	3.5
Rw_F (%)	2.8	4.2
Average shift/error	0.07	0.09

The intensities were corrected for Lorentz and polarisation effects. Scattering factors for neutral atoms and anomalous dispersion corrections for Rh were taken from the *International Tables for X-ray Crystallography* [14]. Both structures were solved by Patterson and Fourier methods. Empirical absorption corrections [15] were applied at the end of isotropic refinements. The maximum and minimum absorption correction factors were 1.135 and 0.918 for **1** and 1.159 and 0.714 for **2**. Final mixed refinement with unit weights and fixed coordinates and the isotropic thermal factors for the hydrogen atoms lead to R values of 2.5% and 3.5% for Tp^{Ph}Rh(NBD) **1** and Tp^{Ph}Rh(COD) **2** respectively. No trends in ΔF vs. F_o or $(\sin\Theta)/\lambda$ were observed. Calculations were performed using the X-ray 80 program [16].

3. Results and discussion

3.1. Synthesis

The potassium salt of the tris(3-phenylpyrazol-1-yl)borate Tp^{Ph-} reacted with the binuclear rhodium complexes $Rh_2Cl_2(NBD)_2$ and $Rh_2Cl_2(COD)_2$ in dry dichloromethane to afford Tp^{Ph}Rh(NBD) **1** and Tp^{Ph}Rh(COD) **2**. Complex $Tp^{Ph}Rh(CO)_2$ **3** was obtained by bubbling a stream of carbon monoxide throughout a dichloromethane solution of **1** or **2**.

3.2. ^1H and ^{13}C NMR spectroscopy

The ^1H NMR data in $CDCl_3$ solution of complex Tp^{Ph}Rh(NBD) **1** show equivalent pyrazolyl rings, δH-4: 6.50 (broad, Fig. 2(a)), δH-5: 7.74 (broad), δCH-1′,4′: 3.08 (broad), δCH-2′,3′,5′,6′: 2.88 (broad), δCH_2-7′: 0.68 (broad), δH_{ortho}: 8.02, ^3J = 8.2 Hz, δH_{meta} and δH_{para}: 7.37–7.54 ppm. This magnetic equivalence is usually explained as corresponding to (i) form **B**, in which a fast exchange between coordinated and free pyrazolyl forms takes place; (ii) form **C**; or even (iii) a fast equilibrium between four- and five-coordinated complexes of types **B** and **C**.

In preceding papers we have established that in $CDCl_3$ the ^{13}C chemical shifts of NBD tetracoordinated complexes follow the sequences: δC-7′ > δC-2′,3′,5′,6′ > δC-1′,4′, and that the δC-2′,3′,5′,6′ appeared at values higher than 58 ppm in tetracoordinated complexes and about 40 ppm in pentacoordinated ones [17–19]. Venanzi and coworkers also pointed out similar criteria in Refs. [6–8].

After recording the ^{13}C NMR spectra in $CDCl_3$ solution, we were able to elucidate between these possibilities; since δC-3: 150.0 (broad), δC-4: 104.0 (broad)

^1J = 176.7, ^2J = 7.0 Hz, δC-5: 136.6 (broad) ^1J = 189.1 Hz, δC-1',4': 49.7 ^1J = 150.0, ^2J(Rh) = 2.4 Hz, *δC-2',3',5',6': 57.0 (broad)* ^1J = 182.2 Hz, δC-7': 61.9, ^1J = 130.4, ^3J(Rh) = 6.2 Hz, δphenyl carbons: 134.0 (C_{ipso}), 127.8, 127.9, 128.1, we conclude that in solution compound **1** exists as a tetracoordinated complex. Moreover, the solid ^{13}C NMR CPMAS chemical shifts, δC-3: 153.4 and 155.3, δC-4: 102.9 and 104.0, δC-5: 136.1 and 137.7, δC-1',4': 48.9 and 50.1, *δC-2',3',5',6': 55.0 and 58.0*, δC-7': 60.7, δphenyl carbons: 127.7, 130.0, 132.0, clearly indicate that its geometry in solution is close to that found in solid state by X-ray crystallography, i.e. a type **B** complex.

The situation is more complicated for compound Tp^{Ph}Rh(COD) **2**, which exists in solution as a mixture of two tetracoordinated forms **A** and **B**. The isomer distribution changes with the polarity of the solvent employed, being 60A/40B in $CDCl_3$ (see Fig. 2(b)), 45A/55B in acetone-d_6 and 34A/66B in DMSO-d_6 at 297 K, and 13A/87B in DMSO-d_6 at 333 K.

Table 2 shows the ^{1}H and ^{13}C NMR chemical shifts for the Tp^{Ph}Rh(COD) complex **2** in $CDCl_3$, with complete assignments to forms **A** and **B** based on symmetry considerations and homo- and heteronuclear correlation experiments [13,20,21].

Here again the ^{13}C chemical shifts for the olefinic carbons of the ancillary ligand COD, in solid CPMAS and in solution, were crucial to confirm that only tetracoordinated forms are present in the Tp^{Ph}Rh(COD) spectra. The *δC-1',2',5',6'* appeared at 78.8 and 83.2 ppm for isomer **A** and 81.2 ppm for isomer **B** in $CDCl_3$ solution, in agreement with a chemical shift of around 80 ppm considered to be normal for the olefinic carbon resonance in four-coordinate Rh–COD complexes [7].

The ^{13}C solid state NMR spectrum of **2** presents four

Table 2
^{1}H and ^{13}C NMR data (chemical shifts, δ in ppm, coupling constants, J in Hz) of complex Tp^{Ph}Rh (COD) (2)

Form A ($CDCl_3$)				
COD				
H-2',5'	*C*-2',5'	*H*-3',4'*exo*	*H*-3',4'*endo*	*C*-3',4'
3.27	78.8 ^1J = 155.4 J(Rh) = 12.4	1.98	1.47	29.9 ^1J = 129.0
H-1',6'	*C*-1',6'	*H*-7',8'*exo*	*H*-7',8'*endo*	C-7',8'
3.89	83.2 ^1J = 155.8 J(Rh) = 12.4	2.44	1.68	30.2 ^1J = 132.4
Pyrazole				
H-4	*C*-4	*H*-5	*C*-5	*C*-3
6.77(1H) ^3J(H-5) = 2.4	102.3(1C) ^1J = 172.9 ^2J = 9.5	8.10(1H)	139.0(1C) ^1J = 185.0	154.0(1C)
6.28(2H) ^3J(H-5) = 2.4	104.8(2C) ^1J = 177.0 ^2J = 8.7	7.44(2H)	135.5(2C) ^1J = 189.9 ^2J = 7.9	154.3(2C)
Form B ($CDCl_3$)				
COD				
H-2',5',1',6'	*C*-2',5',1',6'	*H*-3',4',7',8'*exo*	*H*-3',4',7',8'*endo*	*C*-3',4',7',8'
3.36	81.2 ^1J = 161.7 J(Rh) = 11.1	1.68	1.20	29.1 ^1J = 126.6
Pyrazole				
H-4	*C*-4	*H*-5	*C*-5	*C*-3
6.52(3H) ^3J(H-5) = 2.2	104.8(3C) ^1J = 177.0 ^2J = 8.7	7.81(3H)	137.4(3C) ^1J = 185.0	153.6(3C)
Aryl protons and carbons of forms A and B				
7.28–7.62 (*meta* and *para*, 18H)				
7.96–8.13 (*ortho* protons, 12H)				
125.8, 127.2, 127.7, 127.9, 128.1, 128.2, 128.3, 128.4, 128.6, 133.4, 134.2, 134.5				
^{13}C CPMAS				
Olefinic carbons: 77.0, 80.8, 83.2, 87.9				
Methylene carbons: 25.9, 29.2, 31.9, 32.7				
C-3 pyrazole carbons: 153.6 (broad)			*C*-4 pyrazole carbons: 104.2 (broad)	
C-5 pyrazole carbons: 135.7, 139.1			Aryl carbons: 125.7, 128.0, 132.3	

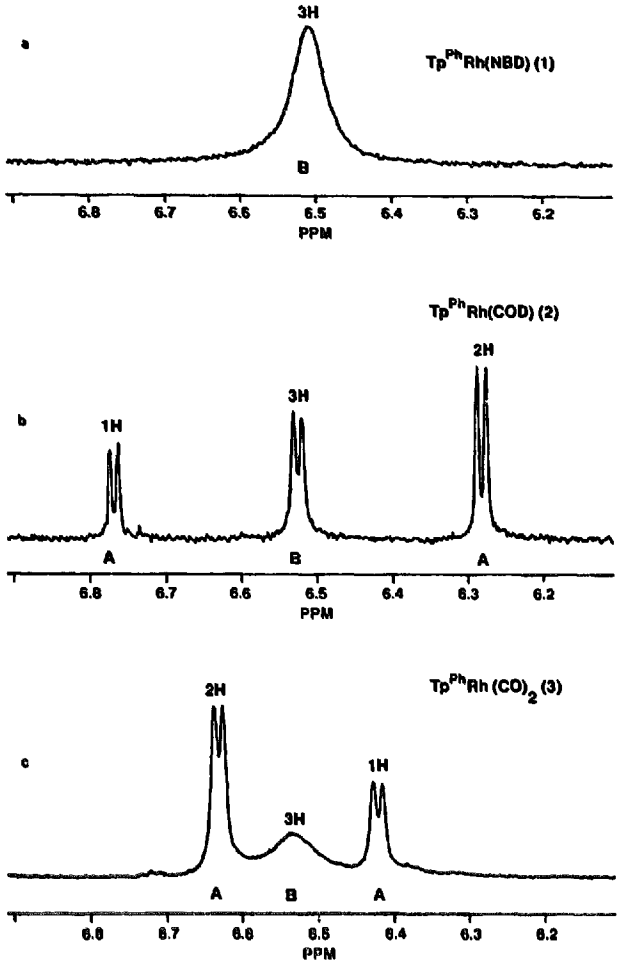

Fig. 2. ^1H NMR region of H-4 in $CDCl_3$ for the three complexes: (a) $Tp^{Ph}Rh(NBD)$ 1; (b) $Tp^{Ph}Rh(COD)$ 2; (c) isomerised sample of $Tp^{Ph}Rh(CO)_2$ 3.

lines for the olefinic carbons at 77.0, 80.8, 83.2 and 87.9, in agreement with the existence of a unique crystallographically independent molecule in the unit cell. The X-ray structure of type **A** shows it to be a tetracoordinated square-planar species formed by the rhodium atom, the two nitrogen atoms of the coordinated pyrazole rings, and the centroids of the double bonds of the COD ligand, with the uncoordinated pyrazole in an *exo*-position with respect to the rhodium atom.

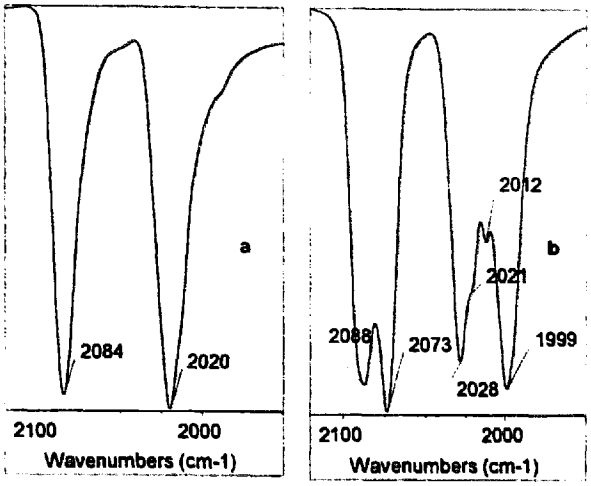

Fig. 3. IR carbonyl stretching frequencies in solid state of: (a) fresh sample of $Tp^{Ph}Rh(CO)_2$ 3; (b) isomerised sample of $Tp^{Ph}Rh(CO)_2$ 3.

A freshly prepared sample of complex $Tp^{Ph}Rh(CO)_2$ 3 in $CDCl_3$ at 297 K shows in ^1H NMR broad resonances for all protons: δH-4: 6.52 (3H *Form B*, broad), δH-5 and δphenyl protons: 7.3–7.8 (18H, broad m), 7.90 (H_{ortho}, d, $^3J = 7.5$ Hz), in agreement with the findings of Krentz [2] (p. 468). This author proposed an equilibrium $k^2 - k^3$ as being responsible for that spectra, in which the major isomer was the four-coordinated one. According to our infrared studies in solid and in solution (see Table 3 and Figs. 3 and 4), our recently obtained sample of $Tp^{Ph}Rh(CO)_2$ 3 presents only bands of a tetracoordinated form at 2089 and 2025 cm^{-1} in carbon tetrachloride, dichloromethane and chloroform (two shoulders appeared in acetonitrile at 2073 and 2012 cm^{-1}).

After three months the foregoing sample of $Tp^{Ph}Rh(CO)_2$ 3 had evolved as deduced from the IR carbonyl bands (Figs. 3 and 4), presenting in ^1H and ^{13}C NMR spectroscopy signals which correspond to forms **A** and **B** in a ratio of 70/30 in $CDCl_3$ at 297 K and 62/38 at 333 K in $CDCl_3$, the chemical shift values

Table 3
Carbonyl stretching bands for complex $Tp^{Ph}Rh(CO)_2$ (3)

	Fresh sample		Evolved sample					
	ν_s	ν_a		ν_s			ν_a	
CCl_4	2088 vs	2025 vs	2091 vs	2078 s		2032 vs	2001 s	
$CHCl_3$	2089 vs	2025 vs	2091 vs	2081 m		2030 m	2006 m	
CH_2Cl_2	2089 vs	2024 vs	2091 vs	2079 vs		2030 vs	2004 vs	
CH_3CN	2089 vs	2025 vs	2090 m	2077 sh	2068 vs	2026 s	2012 sh	1990 vs
	2073 sh	2012 sh						
KBr	2084 vs	2020 vs		2088 vs	2073 vs	2028 vs		
				2021 sh	1999 vs	2012 m		

vs very strong; s strong; m medium; sh shoulder.

being δH-4: 6.42 (1H *Form A*, ^3J = 2.5 Hz), 6.63 (2H *Form A*, ^3J = 2.4 Hz), 6.53 (3H *Form B*, broad) (see Fig. 2(c)), δH-5: 7.17 (1H *Form A*, ^3J = 2.5 Hz), 8.10 (1H *Form A*, ^3J = 2.4 Hz), 8.54 (1H *Form A*, ^3J = 2.4 Hz), δphenyl protons: 7.40–7.63 (m, 18H + $3H_5$ *Form B*), 7.83–8.01 (m, 12H) ppm; δC-3: 156.8, 157.1 ^2J(Rh) = 1.2 Hz and 157.5 ^2J(Rh) = 1.9 Hz, δC-4: 104.7 (vbroad), 105.9 and 106.3, δC-5: 137.6, 140.3 and 137.6, δphenyl carbons: 132.7, 133.0 and 133.2 (C_{ipso}), 128.1, 128.4, 128.5, 128.7, 128.8, 129.4, 129.7, 129.8, δCO: 184.0 ^1J(Rh) = 68.5 Hz, 182.1 ^1J(Rh) = 68.2 Hz, 181.9 ^1J(Rh) = 69.4 Hz, 179.3 ^1J(Rh) = 73.7 Hz. In ^{13}C NMR CPMAS the signals are all very broad, meaning that at least the two forms **A** and **B** coexist in the isomerised solid sample of **3**, δC-3: 156.5, δC-4: 104.9, δC-5: 145, δphenyl carbons: 128.8, 136.1, 137.9, 139.2, δCO: 180–185 ppm.

In acetonitrile-d_3 the ratio **A**/**B** in isomerised **3** is 40/60 by ^{1}H NMR, but by IR it seems that in acetonitrile the three forms are present as deduced from the ν(CO) stretching frequencies (sym and asym) appearing at 2091, 2077, 2026, and 2012 cm^{-1}, characteristic of the two k^2-bidentate species **A** and **B**, and 2068, 1990 cm^{-1} of the k^3-tridentate isomer **C** (see Table 3 and Figs. 3 and 4) [7].

Finally, when comparing the ^{13}C NMR data of the pyrazole groups in complexes **1–3** with those of the trispyrazolylborate ligand Tp^{Ph} [21] a deshielding effect

Table 4
Atomic parameters for [Tp^{Ph}Rh(NBD)] (**1**): coordinates and thermal parameters as $U_{eq} = 1/3\Sigma_i\Sigma_j U_{ij} a_i^* a_j^* a_i \cdot a_j \times 10^4$

Atom	x	y	z	U_{eq}
Rh	0.48075(3)	0.27635(1)	0.88473(2)	3877(8) *
C1	0.4442(4)	0.2559(2)	0.7492(2)	623(14)
C2	0.5763(4)	0.2466(2)	0.7674(2)	615(14)
C3	0.6414(4)	0.3158(3)	0.7508(3)	705(16)
C4	0.5871(5)	0.3573(2)	0.8275(3)	740(17)
C5	0.4547(5)	0.3652(2)	0.8090(3)	737(17)
C6	0.4263(4)	0.3298(3)	0.7200(3)	732(17)
C7	0.5557(5)	0.3423(2)	0.6726(3)	738(17)
B	0.2148(4)	0.2484(2)	0.9893(3)	436(12)
N11	0.3007(3)	0.1833(1)	0.9823(2)	427(9)
N12	0.4158(3)	0.1835(1)	0.9385(2)	420(9)
C13	0.4605(3)	0.1184(2)	0.9380(2)	429(11)
C14	0.3715(4)	0.0762(2)	0.9803(2)	515(12)
C15	0.2732(3)	0.1184(2)	1.0070(2)	492(12)
C16	0.5877(4)	0.1014(2)	0.9005(2)	508(12)
C17	0.6989(4)	0.1388(2)	0.9233(3)	715(16)
C18	0.8193(5)	0.1236(4)	0.8860(4)	1061(26)
C19	0.8270(7)	0.0701(4)	0.8274(5)	1257(33)
C110	0.7175(8)	0.0318(3)	0.8063(4)	1149(28)
C111	0.5967(5)	0.0465(2)	0.8421(3)	753(17)
N21	0.3007(3)	0.3074(1)	1.0297(2)	415(9)
N22	0.4272(2)	0.3193(1)	1.0053(2)	401(8)
C23	0.4754(3)	0.3706(2)	1.0567(2)	429(10)
C24	0.3782(4)	0.3928(2)	1.1128(2)	520(12)
C25	0.2706(3)	0.3517(2)	1.0939(2)	500(12)
C26	0.6154(3)	0.3919(2)	1.0546(2)	450(11)
C27	0.7143(4)	0.3438(2)	1.0457(3)	592(14)
C28	0.8456(4)	0.3640(2)	1.0448(3)	715(16)
C29	0.8789(4)	0.4324(3)	1.0536(3)	702(16)
C210	0.7819(4)	0.4806(2)	1.0628(3)	718(16)
C211	0.6494(4)	0.4610(2)	1.0632(3)	602(14)
N31	0.1593(2)	0.2666(1)	0.8959(2)	433(9)
N32	0.1080(3)	0.3296(1)	0.8782(2)	445(9)
C33	0.0517(3)	0.3258(2)	0.7963(2)	445(11)
C34	0.0657(4)	0.2598(2)	0.7616(2)	594(13)
C35	0.1337(4)	0.2240(2)	0.8265(3)	581(12)
C36	−0.0179(3)	0.3852(2)	0.7568(2)	448(11)
C37	−0.0626(4)	0.4372(2)	0.8106(2)	548(13)
C38	−0.1337(4)	0.4919(2)	0.7740(3)	698(16)
C39	−0.1607(5)	0.4958(3)	0.6848(4)	805(18)
C310	−0.1165(5)	0.4452(3)	0.6308(3)	786(18)
C311	−0.0449(4)	0.3899(2)	0.6654(3)	609(14)

* $U_{eq} \times 10^5$ for the Rh atom.

of the rhodium atom is generally observed for C-3, C-4 and C-5, the coordination induced shifts having increasing values on going from the NBD compound to COD and CO complexes.

3.3. X-ray diffraction study

Tables 4 and 5 show the final atomic parameters for **1** and **2**. A selection of bond lengths and angles, with their standard deviations, is given in Table 6 for both compounds.

The X-ray crystalline structures of $Tp^{Ph}Rh(NBD)$ **1** and $Tp^{Ph}Rh(COD)$ **2** reveal neutral species. As can be observed in the PLUTO views of both molecules shown in Figs. 5 and 6, the rhodium atom in a square-planar coordination mode is bonded to two pyrazolyl rings of the k^2-bidentate hydrotris(3-phenylpyrazol-1-yl)borate ligand Tp^{Ph}, and the centroids of the NBD (C1122, C4455) or COD (C1122, C5566) double bonds (see Table 6).

The rhodium atom is out of that coordination plane by 0.142(1) Å for complex **1** and 0.164(1) Å for complex **2** respectively. The NBD and COD are disposed in an orthogonal orientation with respect to the coordination plane (see Table 7).

This disposition gives a boat conformation metallocycle $Rh(NN)_2B$, as shown in Figs. 5 and 6. The N11, N12, N21, N22 atoms form a plane [22] with a maxi-

Table 5
Atomic parameters for $[Tp^{Ph}Rh(COD)]$ (**2**): coordinates and thermal parameters as $U_{eq} = 1/3\Sigma_i\Sigma_j U_{ij} a_i^* a_j^* a_i \cdot a_j \times 10^4$

Atom	x	y	z	U_{eq}
Rh	0.15691(6)	0.08315(5)	0.39348(2)	365(2)
C1	0.2545(9)	−0.0405(7)	0.3485(3)	486(29)
C2	0.2105(8)	−0.1103(7)	0.3827(3)	475(27)
C3	0.3055(10)	−0.1535(9)	0.4207(3)	657(36)
C4	0.4056(9)	−0.0538(11)	0.4365(3)	656(37)
C5	0.3427(9)	0.0795(9)	0.4327(2)	530(25)
C6	0.3642(8)	0.1569(8)	0.3976(3)	560(28)
C7	0.4405(10)	0.1246(9)	0.3563(4)	685(38)
C8	0.4069(11)	−0.0036(9)	0.3387(4)	601(36)
B	0.0217(9)	0.2864(9)	0.3317(3)	407(28)
N11	−0.0650(7)	0.1604(6)	0.3327(2)	385(20)
N12	−0.0373(6)	0.0677(6)	0.3618(2)	383(19)
C13	−0.1362(8)	−0.0238(7)	0.3555(3)	377(23)
C14	−0.2208(8)	0.0107(8)	0.3209(3)	445(26)
C15	−0.1739(9)	0.1256(8)	0.3075(2)	445(25)
C16	−0.1574(9)	−0.1266(6)	0.3877(2)	391(21)
C17	−0.1130(10)	−0.1184(8)	0.4292(3)	550(31)
C18	−0.1450(12)	−0.2102(8)	0.4592(3)	620(32)
C19	−0.2251(12)	−0.3130(9)	0.4467(3)	716(39)
C110	−0.2693(12)	−0.3230(9)	0.4034(3)	681(36)
C111	−0.2347(11)	−0.2306(7)	0.3755(4)	717(37)
N21	0.0369(7)	0.3340(6)	0.3797(2)	439(21)
N22	0.0813(6)	0.2590(6)	0.4133(2)	388(20)
C23	0.0863(9)	0.3315(8)	0.4485(3)	421(27)
C24	0.0519(10)	0.4540(7)	0.4378(3)	542(30)
C25	0.0190(9)	0.4523(7)	0.3940(3)	509(26)
C26	0.1191(8)	0.2782(7)	0.4920(2)	396(26)
C27	0.1962(8)	0.3457(8)	0.5212(2)	473(28)
C28	0.2242(10)	0.2962(10)	0.5616(3)	605(34)
C29	0.1735(10)	0.1785(9)	0.5732(3)	597(32)
C210	0.0914(9)	0.1117(9)	0.5441(3)	545(31)
C211	0.0665(10)	0.1608(8)	0.5035(3)	507(29)
N31	−0.0618(7)	0.3825(6)	0.3068(2)	463(23)
N32	−0.1976(6)	0.4114(8)	0.3168(2)	478(21)
C33	−0.2352(11)	0.5060(8)	0.2916(3)	526(30)
C34	−0.1218(12)	0.5369(9)	0.2635(3)	732(39)
C35	−0.0154(11)	0.4593(9)	0.2750(3)	606(33)
C36	−0.3788(10)	0.5568(8)	0.2929(3)	535(30)
C37	−0.4149(13)	0.6665(9)	0.2704(3)	755(41)
C38	−0.5473(16)	0.7160(11)	0.2732(4)	890(55)
C39	−0.6443(15)	0.6582(14)	0.2968(5)	1023(59)
C310	−0.6158(11)	0.5492(13)	0.3201(4)	925(52)
C311	−0.4814(12)	0.4996(11)	0.3174(4)	747(41)

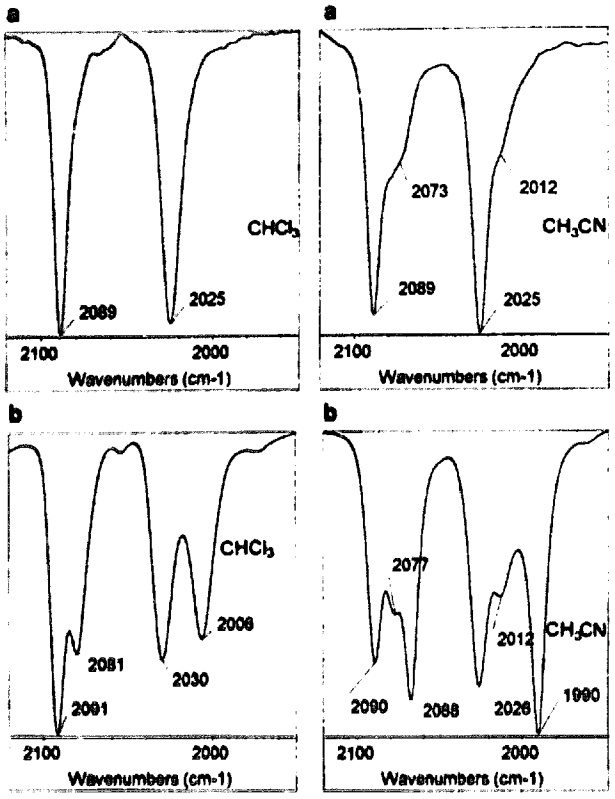

Fig. 4. IR carbonyl stretching frequencies in solution of: (a) fresh sample of $Tp^{Ph}Rh(CO)_2$ **3** in $CHCl_3$ and CH_3CN; (b) isomerised sample of $Tp^{Ph}Rh(CO)_2$ **3** in $CHCl_3$ and CH_3CN.

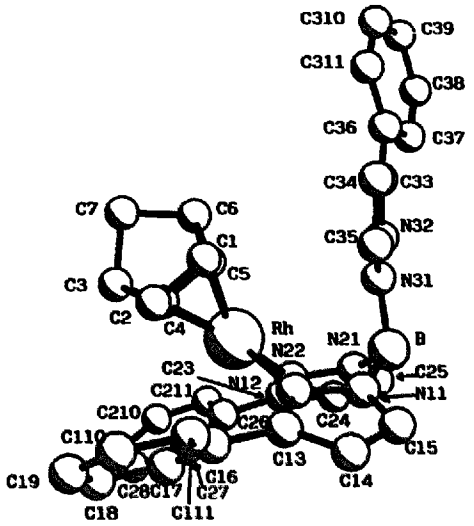

Fig. 5. A PLUTO plot of $Tp^{Ph}Rh(NBD)$ **1**. The atom C29 is eclipsed by C110. The hydrogen atoms have been omitted.

mum deviation of 0.061(3) Å in $Tp^{Ph}Rh(NBD)$ **1** and 0.017(7) Å in $Tp^{Ph}Rh(COD)$ **2** for N11. Rh and B atoms are out of this plane at distances of 1.0383(4) and 0.567(4) Å for compound **1** and 1.1747(9) and 0.574(9) Å for **2**.

The main difference between both k^2-bidentate Tp^{Ph} complexes is the spatial orientation of the uncoordinated

Table 6
Selected bond distances (Å) and angles (°) for $[Tp^{Ph}Rh(NBD)]$ (**1**) and $[Tp^{Ph}Rh(COD)]$ (**2**) with esds in parentheses

(1)		(2)	
Rh–C1	2.093(4)	Rh–C1	2.126(9)
Rh–C2	2.128(4)	Rh–C2	2.145(8)
Rh–C4	2.111(5)	Rh–C5	2.140(8)
Rh–C5	2.081(4)	Rh–C6	2.122(8(
Rh–N12	2.096(3)	Rh–N12	2.094(6)
Rh–N22	2.091(3)	Rh–N22	2.094(6)
Rh–C1122	1.998(3)	Rh–C1122	2.025(8)
Rh–C4455	1.893(3)	Rh–C5566	2.018(8)
C1–C2	1.361(6)	C1–C2	1.357(12)
C4–C5	1.362(8)	C5–C6	1.377(12)
B–N11	1.542(5)	B–N11	1.572(11)
B–N21	1.548(5)	B–N21	1.573(10)
B–N31	1.530(5)	B–N31	1.505(11)
N12–Rh–N22	84.97(10)	N12–Rh–N22	84.56(24)
N12–Rh–C4455	170.88(12)	N12–Rh–C5566	169.8(3)
N12–Rh–C1122	102.71(13)	N12–Rh–C1122	92.7(3)
N22–Rh–C4455	99.77(13)	N22–Rh–C5566	93.1(3)
N22–Rh–C1122	168.12(12)	N22–Rh–C1122	171.6(3)
C4455–Rh–C1122	71.42(14)	C1122–Rh–C5566	88.2(3)
C4–Rh–C5	37.90(17)	C5–Rh–C6	37.7(3)
C1–Rh–C2	37.63(15)	C1–Rh–C2	37.0(3)

C1122, C4455 and C5566 are the midpoints of C1, C2; C4, C5; and C5, C6 respectively.

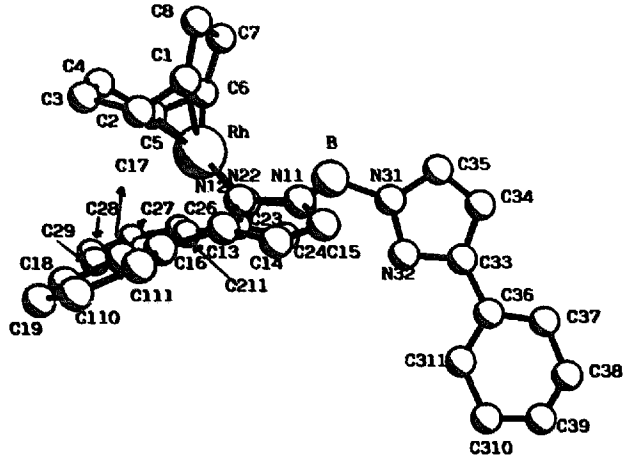

Fig. 6. A PLUTO plot of $Tp^{Ph}Rh(COD)$ **2**. The atoms C25 and N21 are eclipsed by C15 and N11. The hydrogen atoms have been omitted.

pyrazole, in $Tp^{Ph}Rh(NBD)$ **1** it occupies an axial position, a typical example of a four-coordinate species of type **B**. On the contrary, in $Tp^{Ph}Rh(COD)$ **2** an **A** form, the non-coordinating pyrazole, appears in an equatorial position, similarly to what has been described for $Tp^{Ph}Rh(CO)_2$ **3** [2]. The distances Rh–N31 are 3.263(3) and 4.649(7) Å and Rh–B 3.218(4) and 3.156(9) Å for complexes **1** and **2** respectively.

One striking difference between complexes **1** and **2** is observed in the boron–nitrogen distances: in form **A** of $Tp^{Ph}Rh(COD)$ **2**, B–N11 and B–N21 have a value of 1.57(1) Å and B–N31 is 1.50(1) Å, meanwhile in form **B** of $Tp^{Ph}Rh(NBD)$ **1** the three distances are close to approximately 1.54(5) Å.

4. Conclusions

The coordination mode of hydrotris(3-phenylpyrazol-1-yl)borate ligand, Tp^{Ph}, in Rh(I) complexes of type $Tp^{Ph}Rh(LL)$ [LL = NBD, COD, $(CO)_2$] **1–3** has been studied. In the solid state, X-ray crystallography, IR and ^{13}C CPMAS spectroscopy reveal the k^2-denticity of the chelating ligand in $Tp^{Ph}Rh(NBD)$ **1** and $Tp^{Ph}Rh(COD)$ **2**, in agreement with the previously known structure of $Tp^{Ph}Rh(CO)_2$ **3**.

In solution a dynamic equilibrium between two isomeric forms is evidenced for complexes $Tp^{Ph}Rh(COD)$ **2** and *evolved* $Tp^{Ph}Rh(CO)_2$ **3**: **A**, a tetracoordinate square-planar complex with two coordinated pyrazolyl groups and the uncoordinated one in equatorial position; **B**, a tetracoordinate square-planar complex with two coordinated pyrazoles and the third one in axial position. In both cases an increase in temperature as well as polarity of the solvent shifted the equilibrium towards the tetracoordinated form **B**. For complex $Tp^{Ph}Rh(NBD)$ **1** only **B** was detected in solution.

Finally, in the isomerised sample of $Tp^{Ph}Rh(CO)_2$ **3**, IR studies suggested that in a polar solvent such as acetonitrile form **C** is also present.

We conclude that, in hydrotrispyrazolylborate ligands, large substituents in the 3-position of the pyra-

Table 7
Selected angles (°) between the least-squares sets defined by the specified atoms for (1) and (2)

(1)		(2)
planes		*planes*
1	N12, N22, C1122, C4455	N11, N22, C1122, C5566
2	C1, C2, C4, C5	C1, C2, C5, C6
3	N11, N12, C13, C14, C15	N11, N12, C13, C14, C15
4	N21, N22, C23, C24, C25	N21, N22, C23, C24, C25
5	N31, N32, C33, C34, C35	N31, N32, C33, C34, C35
6	C16, C17, C18, C19, C110, C111	C16, C17, C18, C19, C110, C111
7	C26, C27, C28, C29, C210, C211	C26, C27, C28, C29, C210, C211
8	C36, C37, C38, C39, C310, C311	C36, C37, C38, C39, C310, C311
1–2	83.61(16)	83.3(3)
1–3	46.55(10)	59.09(24)
1–4	53.43(12)	55.7(3)
1–5	48.21(9)	80.90(23)
1–6	59.87(12)	77.2(3)
1–7	69.08(10)	70.07(23)
1–8	45.60(11)	71.63(23)
3–4	50.05(12)	50.2(3)
3–5	83.26(11)	58.1(3)
4–5	79.64(12)	72.52(3)
3–6	48.91(12)	26.7(3)
4–7	40.03(12)	38.8(3)
5–8	21.10(13)	9.3(3)

C1122, C4455, C5566 are the midpoints of C1, C2; C4, C5; and C5, C6 respectively.

zolyl group (as phenyl Ph) disfavor the formation of the k^3-coordinated species of type C.

Acknowledgements

We are indebted to DGICYT of Spain for financial support (Project Nos. PB93-0197-C02 and PB92-0213) and Comunidad de Madrid (Acciones Especiales AE00067/95 and AE111/95). The FT-IR Nicolet Magna 550 spectrometer was purchased thanks to the DGICYT of Spain (Mat95-0940-E).

References

[1] S. Trofimenko, *Chem. Rev.*, *93* (1993) 943.
[2] N. Kitajima and W.B. Tolman, *Progr. Inorg. Chem.*, *43* (1995) 419.
[3] G. Parkin, *Adv. Inorg. Chem.*, *42* (1995) 291; M.C. Kuchta, H.V. Rasika Dias, S.G. Bott and G. Parkin, *Inorg. Chem.*, *35* (1996) 943.
[4] W.M. Vaughan, K.A. Abboud and J.M. Boncella, *J. Organomet. Chem.*, *485* (1995) 37; G.G. Lobbia, P. Cecchi, R. Spagna, M. Colapietro, A. Pifferi and C. Pettinari, *J. Organomet. Chem.*, *485* (1995) 45; S.J. Mason, C.M. Hill, V.J. Murphy, D. O'Hare and D.J. Watkin, *J. Organomet. Chem.*, *485* (1995) 165; V.S. Joshi, K.M. Sathe, M. Nandi, P. Chakrabarti and A. Sarkar, *J. Organomet. Chem.*, *485* (1995) C1.
[5] A.L. Rheingold, C.B. White and S. Trofimenko, *Inorg. Chem.*, *32* (1993) 3471; J. Huang, L. Lee, B.S. Haggerty, A.L. Rheingold and M. Walters, *Inorg. Chem.*, *34* (1995) 4268.
[6] U.E. Bucher, Th.F. Fässler, M. Hunziker, R. Nesper, H. Rüegger and L.M. Venanzi, *Gazz. Chim. Ital.*, *125* (1995) 181.
[7] U.E. Bucher, A. Currao, R. Nesper, H. Rüegger, L.M. Venanzi and E. Younger, *Inorg. Chem.*, *34* (1995) 66.
[8] E. Del Ministro, O. Renn, H. Rüegger, L.M. Venanzi, U. Burckhardt and V. Gramlich, *Inorg. Chim. Acta*, *240* (1995) 631.
[9] J. Elguero and R. Jacquier, *Bull. Soc. Chim. Fr.*, (1966) 2832.
[10] S. Trofimenko, J.C. Calabrese and J.S. Thompson, *Inorg. Chem.*, *26* (1987) 1507.
[11] E.W. Abel, M.A. Bennett and G. Wilkinson, *J. Chem. Soc. A*, (1959) 3178.
[12] J. Chatt and L.M. Venanzi, *J. Chem. Soc.*, (1957) 4735.
[13] W.R. Croasmun and R.M.K. Carlson, *Two-Dimensional NMR Spectroscopy*, VCH, Weinheim, 2nd edn., 1994.
[14] *International Tables for X-ray Crystallography*, Vol. 4, Kynoch Press, Birmingham, 1974, pp. 72–98.
[15] N. Walker and D. Stuart, *Acta Crystallogr., A39* (1983) 158.
[16] J.M. Stewart, *The X-ray 80 system*, Computer Science Center, University of Maryland, College Park, MD, 1985.
[17] M.C. López Gallego-Preciado, P. Ballesteros, R.M. Claramunt, M. Cano, J.V. Heras, E. Pinilla and A. Monge, *J. Organomet. Chem.*, *450* (1993) 237.
[18] P. Ballesteros, C. López, R.M. Claramunt, J.A. Jiménez, M. Cano, J.V. Heras, E. Pinilla and A. Monge, *Organometallics*, *13* (1994) 289.
[19] C. López, J.A. Jiménez, R.M. Claramunt, M. Cano, J.V. Heras, J.A. Campo, E. Pinilla and A. Monge, *J. Organomet. Chem.*, *511* (1996) 115.
[20] C. López, R.M. Claramunt, D. Sanz, C. Foces-Foces, F.H. Cano, R. Faure, E. Cayón and J. Elguero, *Inorg. Chim. Acta*, *176* (1990) 195.
[21] C. López, D. Sanz, R.M. Claramunt, S. Trofimenko and J. Elguero, *J. Organomet. Chem.*, *503* (1995) 265.
[22] M. Nardelli, A. Musatti, P. Domiano and G.D. Andreetti, *Ric. Sci. Part 2, Sect. A*, *8* (1965) 807.